Article for consideration by Oecologia

Spectral determination of concentrations of functionally diverse pigments in increasingly complex arctic tundra canopies

Natalie T. Boelman[1,*], Troy S. Magney [2], Barry A. Logan[3], Kevin L. Griffin[1], Jan U.H. Eitel [2,4], Heather Greaves[2], Case M. Prager[5], and Lee A. Vierling [2,4]

[1] Lamont-Doherty Earth Observatory, Columbia University, New York, NY, USA, 10964

[2] Geospatial Laboratory for Environmental Dynamics, University of Idaho, Moscow, ID, USA 83844-1133;

[3] Department of Biology, Bowdoin College, Brunswick, ME, USA, 04011

[4] McCall Outdoor Science School, University of Idaho, McCall, ID, USA, 83638

[5] Department of Ecology, Evolution, and Environmental Biology, Columbia University, New York, NY, USA, 10027

*Author to whom correspondence should be addressed; E-Mail: nboelman@ldeo.columbia.edu; Tel.: +1-845-365-8480

Declaration of authorship: NTB, TSM, BAL, KLG, JUHE, HG, CMP and LAV co-conceived, designed and executed this study. NTB collected and analyzed the spectral datasets while TSM and BAL conducted the pigment laboratory analyses. NTB wrote the manuscript with feedback on a previous draft from all other co-authors.

ABSTRACT. As the Arctic warms, tundra vegetation is becoming taller and more structurally complex as tall deciduous shrubs become increasingly dominant. Emerging studies reveal that shrubs exhibit photosynthetic resource partitioning, akin to forests, that may need accounting for in "big leaf" net ecosystem exchange models. We conducted a lab experiment on sun and shade leaves from *S. pulchra* shrubs to determine the influence of both constitutive (slowly changing bulk carotenoid and chlorophyll pools) and facultative (rapidly changing xanthophyll cycle) pigment pools on a suite of spectral vegetation indices, to devise a rapid means of estimating within canopy resource partitioning. We found that: (1) the PRI of dark-adapted shade leaves (PRI_o) was double that of sun leaves, and that PRI_o was sensitive to variation among sun and shade leaves in both xanthophyll cycle pool size (V+A+Z) (r^2=0.59) and Chl*a*/*b* (r^2=0.64); (2) A corrected PRI (difference between dark and illuminated leaves, ΔPRI) was more sensitive to variation among sun and shade leaves in changes to the epoxidation state of their xanthophyll cycle pigments (dEPS) (r^2=0.78, RMSE=0.007) compared to the uncorrected PRI of illuminated leaves (PRI) (r^2=0.34, RMSE=0.02) and; (3) the SR680 index was correlated with each of (V+A+Z), lutein, bulk carotenoids, (V+A+Z)/(Chl*a*+*b*), and Chl*a*/*b* (r^2 range=0.52-0.69). We suggest that ΔPRI be employed as a proxy for facultative pigment dynamics, and the SR680 for estimation of constitutive pigment pools. We contribute the first Arctic-specific information on disentangling PRI-pigment relationships, and offer insight into how spectral indices can assess resource partitioning within shrub tundra canopies.

Keywords. resource partitioning; PRI; ΔPRI; remote sensing; shrubs; xanthophyll cycle

INTRODUCTION. It is projected that as the Arctic continues to warm, tundra vegetation cover will shift from being composed primarily of low-lying vegetation to dominance by tall deciduous shrubs and even tree cover mosaics (Hallinger et al. 2010, Fraser et al. 2011, Macias-Fauria et al. 2012, Pearson et al. 2013). This compositional shift has already begun in many regions (Stow et al. 2004, Tape et al. 2006, Myers-Smith et al. 2011 and 2015, Loranty and Goetz 2012, Elmendorf et al. 2012), and will result in tundra ecosystems having not only greater vegetation biomass and higher leaf area index values (LAI) (Street et al. 2007, McManus et al. 2012), but also taller and more structurally complex vegetation (Walker et al. 2006, Boelman et al. 2011). Evidence is accumulating that shows that these concurrent shifts in tundra structure are accompanied by changes in tundra function, including in the exchange of carbon between its vegetation and the atmosphere (Shaver et al. 2007, Street et al. 2007, Sweet et al. 2015). Because tundra regions are vast, remote, and play a critical role in the global carbon cycle (McGuire et al. 2009), it is important to develop and use the appropriate tools and models that enable accurate monitoring of its carbon dynamics.

Shaver et al. (2007) showed that tundra net ecosystem productivity (NEE) can be estimated by combining information on only three variables: LAI, incoming photosynthetically active radiation (PAR), and ambient air temperature. This arctic tundra specific "big leaf model" (Field et al. 1991) has been widely successful for predicting NEE (Williams and Rastetter 1999, Sweet et al. 2015) because the vast majority of present day tundra is short and structurally simple, so that light attenuation, and thus resource partitioning *within* tundra canopies is negligible (Williams et al. 2001, 2008). To boot, because present day tundra typically has LAI values less than 1, the widely employed normalized difference vegetation index (NDVI, Rouse et al. 1974) can be used to remotely estimate spatial and temporal dynamics in LAI for inclusion in

68 the model (Street et al. 2007). However, emerging studies by Magney et al. (*in press*) reveal that
69 within canopy resource partitioning according to within canopy variation in light environment
70 (self-shading) - akin to that of forested ecosystems (Niinemets 2003, 2007, 2010) - is already
71 occurring in tall deciduous shrubs. Specifically, these studies show that present day shrub-
72 dominated tundra canopies include a wide range of light environments, from deeply shaded
73 regions with lower investment in nitrogen as well as photosynthetic and photoprotective
74 capacities, relative to highly sun exposed regions with higher nitrogen and chlorophyll pigment
75 investments (Magney et al. *in review*). Such gradients will be enhanced as the tundra continues
76 to grow taller and more structurally complex, resulting in two major consequences for future
77 estimation of tundra NEE. First, tundra models will need to be modified to include
78 photosynthetic resource partitioning within vegetation canopies. Second, traditional spectral
79 vegetation indices alone, such as NDVI, are insensitive to rapidly changing (facultative) pigment
80 pools (i.e. those that govern the xanthophyll cycle conversion state) that control diurnal and
81 seasonal dynamics in photosynthesis. Thus, complementary approaches may prove necessary for
82 scaling canopy level photosynthesis (Gamon et al. 1995,2001,2015, Asner et al. 2004, Gitelson
83 et al. 2006, Hall et al. 2008, Peñuelas et al. 2011) in NEE models to the greater tundra
84 ecosystem.

85 Over the past two decades, there has been increasing interest in the use of the
86 photochemical reflectance index (PRI, Gamon et al. 1990,1992) - a narrowband spectral
87 reflectance index - for quantifying leaf to stand-level dynamics in photosynthetic activity and
88 canopy light-use efficiency (LUE) (Gamon et al. 1992,2001). Together, a suite of leaf pigments
89 enable plants to absorb light essential to photosynthesis, but also dissipate excess light energy in
90 the form of heat (Butler 1978, Demmig-Adams and Adams 1996). These photoprotective

91 mechanisms provide means by which plants can avoid sustained reductions in rates and
92 efficiency of photosynthesis (photoinhibition) (Powles 1984), as well as damage to
93 photosynthetic apparatus (Niyogi 2000, Erickson et al. 2015). PRI takes advantage of the fact
94 that reflectance at 531 nm is functionally related to rapid conversions between epoxidation states
95 of the xanthophyll cycle carotenoids (Gamon et al. 1990,1992) which are linked to foliar heat
96 dissipation (Demmig-Adams and Adams 1996) and thus photosynthetic LUE. However, PRI has
97 proven sensitive not only to dynamics in photoprotective pigment conversion states, but also to
98 longer-term investment in various pigment pools which are also important determinants of
99 photosynthetic LUE (Gamon et al. 1990,1992, Penuleas et al. 1995, Filella et al. 1996, Garbulsky
100 et al. 2011, Gamon and Berry 2012). Gamon and Berry (2012) have termed these pigment pools
101 *facultative* and *constitutive* pigment pools, respectively, because while the inter-conversion
102 between epoxidation states of the xanthophyll cycle carotenoids enables rapid, facultative
103 adjustments in leaves under varying light stress conditions (i.e. seconds to minutes) (Demmig-
104 Adams and Adams 1992, Hartel et al. 1999, Peguero-Pina et al. 2013), investment in bulk
105 carotenoid pools govern the longer-term constitutive capacity of foliage to dissipate excess
106 energy (i.e. weeks to months) (Demmig-Adams 1998). Due to the sensitivity of PRI to dynamics
107 in both constitutive and facultative pigment pools, disentanglement of their dual influence has
108 been a challenge only recently overcome by a suite of PRI studies conducted both at the leaf and
109 stand-levels in a variety of tropical, temperate and boreal ecosystems (Garrity et al. 2011, Gamon
110 and Berry 2012, Porcar-Castell et al. 2012, Rahimzadeh-Bajgiran et al. 2012, Hmimina et al.
111 2014,2015, Najaki et al. 2006, Gamon et al. 2015, Wong and Gamon 2015a,b). As such, unlike
112 other vegetation indices, PRI offers the unique potential to quantify dynamics in both

113 constitutive and facultative pigment pools, thereby providing insight into photosynthetic
114 efficiency at a wide range of temporal scales.
115 To our knowledge, neither PRI nor any other spectral index has been explored as a means
116 of studying *within* canopy pigment dynamics in arctic tundra, or elsewhere. Further, while
117 countless other spectral vegetation indices have been developed and successfully employed at the
118 leaf level to characterize relatively large, slow changes in constitutive pigment pools (as
119 reviewed by Blackburn et al. 2007 and Ustin et al. 2009), there has been far less focus on
120 exploring their sensitivity to the much smaller range in more facultative pigment pool dynamics
121 that Magney et al. (*in review*) have recently discovered within arctic shrub canopies during the
122 period of maximum canopy greenness. While examination of differences in xanthophyll cycle
123 activity within shrub canopies is the primary focus of Magney et al. (*in review*), the main goal of
124 the current study is to explore the potential use of spectroscopy to study within canopy dynamics
125 in both constitutive and facultative pigment pools. As such, our three objectives are to expand on
126 previous work by determining the following for one of the most ubiquitous and rapidly
127 expanding deciduous shrub species in arctic Alaska – *Salix pulchra*: (1) if and how the PRI is
128 responsive to differences in constitutive pigment pools among leaves from naturally varying
129 canopy positions and light histories; (2) if and how the PRI is responsive to dynamics in
130 facultative pigment pools (xanthophyll cycle conversion state) in response to a dark to light
131 transition, and; (3) if and how a suite of other vegetation indices are responsive to differences
132 between sun and shade leaves in their constitutive pigment pools in order to determine how they
133 may potentially complement PRI as a means of rapidly estimating resource partitioning with
134 shrub canopies. Based on findings of previous work in other ecosystems we hypothesized that:
135 (1) PRI of dark adapted leaves would be sensitive to differences in both constitutive bulk and

individual carotenoid pool sizes and carotenoid to chlorophyll ratios, with lower PRI values (indicating higher xanthophyll pigment pools) in sun compared to shade leaves; (2) PRI of leaves would be sensitive to changes in xanthophyll cycle epoxidation state that occur during a dark to light transition, with sun leaves exhibiting lower PRI values than shade leaves under illuminated measurement conditions, and; (3) A suite of spectral vegetation indices that have been previously shown to vary with foliar pigment pools would be sensitive to differences in constitutive pigment pools between sun and shade leaves.

MATERIALS AND METHODS.

Arctic study site. This study took place in the Northern Alaska tundra at the Arctic Long Term Ecological Research (LTER) site at Toolik Lake (68.63°N, -149.60°W) during peak growing season (July 6-16) of 2014, during which time daily average temperatures ranged from 8 - 17 °C. Leaves from *Salix pulchra* were examined, as this is one of the primary shrub species attributed to climate-induced shrub expansion in the Arctic (Myers-Smith et al. 2011). The mean height of studied shrubs was ~ 1 m, and samples were taken from four shrubs located in a shrub tundra community in the vicinity of Toolik Field Station. This ecosystem is dominated by deciduous shrubs (*S. pulchra, S. alaxensis, Betula nana)* and graminoids (primarily *Eriophorum vaginatum-Sphagnum* and *Carex bigelowii-Sphagnum*), and average soil pH < 5.5. The mean annual air temperature for this region is -8.7° C and mean annual precipitation is 164.5 mm.

Experimental approach. We collected branches that included sun and shade leaves from four *Salix pulchra* individuals (see 'Leaf sample collection'). All leaves were dark-acclimated for > 2 hrs to allow for the relaxation of thermal energy dissipation consequent with the epoxidation of the xanthophyll cycle carotenoids. Following dark-acclimation, branches were placed in a very

dim (< 10 μmol m-2 s-1) light environment while spectral reflectance measurements (using a light source internal to the spectroradiometer) and leaf samples were collected for pigment extractions. Similar to Gamon and Berry (2012), we used dark- acclimated leaves in an initial set of pigment and PRI measurements to experimentally separate the influence of foliar *investment* in pigments (i.e. a function of the constitutive pigment pools) from the influence of *activity* of xanthophyll cycle pigments (i.e. a function of the facultative pigment pools) on PRI (Gamon and Berry 2012) because in measuring dark-acclimated leaves, the experimentally induced dark state (epoxidation to violaxanthin in the dark) minimized the influence of light controlled xanthophyll cycle activity on the measured PRI. Thus, under these conditions, PRI variation among leaves was primarily due to differences in the investment of bulk pigment pool composition, and secondarily due to small differences in the amount of ambient (but dim) light each leaf sample was exposed to and may have influenced xanthophyll cycle activity. Hereafter we refer to this dark-state PRI measurement as PRI_o.

Following the dark-acclimated leaf measurements for determining pigment spectral reflectance, each branch was placed under a bank of lights (high-intensity discharge metal halide lamps) facing directly towards the leaves to induce xanthophyll pigment interconversion. Leaf level irradiance ranged from 200 μmol m^{-2} s^{-1} to 1200 μmol m^{-2} s^{-1}. The range in light exposure was the result of varying leaf angles on the stem, and was quantified as photosynthetic photon flux density (PPFD) measured by a quantum sensor. After exposure to light for more than three minutes, it was assumed that xanthophyll de-epoxidation had occurred (Bilger et al. 1989). At this time, a second set of pigment samples were taken and spectral reflectance measurements were made, both from the same leaves sampled under dark state conditions. Hereafter we refer to the PRI measurements made under high light intensities as PRI.

Leaf sample collection. A total of eight *Salix pulchra* branches (4 sun exposed, 4 shaded) from four different shrubs were collected in the field from which a total of 40 leaf samples encompassing 20 sun-exposed leaves and 20 shade leaves were analyzed. All branches sampled had leaves that were fully expanded and were chosen subjectively to ensure that representative sun and shade leaves were chosen. Sun/shade conditions were quantified using a plant canopy analyzer (LAI-2000, LiCor, Lincoln, NE, USA), and data was collected during diffuse sky conditions to reduce sun/sensor geometry effects (Bréda et al. 2003). LAI values ≤ 0.3 were considered sun leaves, while LAI values > 0.3 were considered shade leaves. All branches were taken back to the laboratory. The leaves remained attached to branches, and the branch was placed in ample water and re-cut.

Pigment analysis. A 0.25 cm^2 disk of leaf tissue was removed from each dark-acclimated and illuminated leaf using a cork borer and immediately were stored at -80°C until extraction in acetone according to Adams and Demmig-Adams (1992). Pigment separation and quantification were achieved by high-performance liquid chromatography (HPLC), as described in Gilmore and Yamamoto (1991), using an Agilent 1100 series HPLC (Agilent Technologies, Palo Alto, CA, USA) equipped with a YMC Carotenoid C-30 reverse phase column (YMC Co., Ltd, Kyoto, Japan) at 35°C with the following modification to the solvent gradient: 0–4 min (72 : 8 : 3, acetonitrile : methanol : 0.1MTris-HCl (pH 8.0)) followed by a linear gradient to 80% (4 : 1, methanol : hexanes) from 4 to 40 min, and the completion of the quantification with the latter mobile phase. Pigment pool sizes quantified were: chlorophyll a (Chl*a*) and b (Chl*b*) (in $mmol/m^2$), and individual carotenoid pool sizes (in $\mu mol/m^2$): violaxanthin (V), antheraxanthin (A), zeaxanthin (Z), neaxanthin, lutein, and beta-carotene. Several of these individual pigment values were combined to calculate the total chlorophyll pool size (Chl*a*+*b*=Chl*a*+Chl*b*) (in

mmol/m^2), total xanthophyll cycle pool size (V+A+Z) (in μmol/m^2), bulk carotenoid pool size (bulk car = V+A+Z+neaxanthin+lutein+beta-carotene) (in μmol/m^2). In addition, several pigment ratios were calculated: Chl*a/b*, (bulk car)/(Chl*a*+*b*) (in mmol mol^{-1}), (V+A+Z)/(Chl*a*+*b*) (in mmol mol^{-1}), and lutein/(Chl*a*+*b*) (in mmol mol^{-1}). The xanthophyll cycle pigment epoxidation state (EPS) is the ratio of the epoxidised to the de-epoxidised components of the xanthophyll cycle (EPS=(V+0.5A)/(V+A+Z)) because of the involvement of zeaxanthin and antheraxanthin in the energy dissipation process (Gilmore and Yamamoto 1993). A weighting factor of 0.5 is applied to antheraxanthin since it is only a partially de-epoxidized relative to violaxanthin (Thayer and Björkman 1990). The change in EPS from the dark to light transition (dEPS) was calculated as the difference between the EPS of light and dark acclimated leaves. Of the pigment pools listed above, the following are reported in related study by Magney et al. (*in press, in review*), and also included in the current study in order to relate pigment pools to a suite of narrowband spectral vegetation indices: Magney et al., *in press: Chla/*b; Magney et al., *in review:* (V+A+Z)/(Chl*a*+*b*); (Z+A)/(V+A+Z).

Spectral reflectance: PRI and other vegetation indices. Leaf spectral radiance measurements were made on dark-acclimated and illuminated leaves (immediately following and on the same leaves from which pigment samples were removed) using a spectroradiometer (UniSpec SC, PP Systems, Haverhill MA, USA) by attaching a fiber optic probe (UNI400, PP Systems, Haverhill MA, USA) onto a leaf with a leaf clip (UNI500, PP Systems, Haverhill MA, USA). The fiber optic probe includes both a white measuring and actinic light (PPFD equal to full sun), and a path for reflected light to reach the detector (see Gamon and Surfus 1999, for further details and instrument description). The leaf clip provided a fixed optical geometry during spectral sampling. The spectral sampling range was 310 - 1100 nm, with a sampling interval of 3.3 nm,

and full-width half maximum bandwidth of 10 nm for a total of 256 data points per spectrum. Leaf radiance measurements were preceded by: (1) a 'dark spectrum' in which the spectroradiometer light source is blocked (by a shutter) from reaching the leaf clip. The spectrum from the dark spectrum is used by the spectroradiometer to correct for instrument noise, and (2) a measurement of a 99% reflectance white standard (Spectralon, LabSphere, North Sutton, NY, USA). The integration time was set to 15 ms. Three spectral measurements were made per leaf sample to ensure that the spatial heterogeneity of each leaf region was captured. All spectral measurements were converted to reflectance values by dividing each leaf measurement by the white standard measurement. All reflectance spectra were interpolated using a linear interpolation to a 1 nm interval so that narrowband vegetation indices that require single wavelength reflectance values could be calculated. Several narrowband vegetation indices that have proven effective at estimating foliar pigment contents across a range of species, growth forms, spatial and temporal scales, were then calculated according the equations in Table 1. In addition, three different PRI values were calculated: (1) PRI_o indicates values calculated from reflectance measurements made on dark-acclimated leaves, (2) PRI indicates values calculated from reflectance measurements made on leaves exposed to high light intensities; and; (3) ΔPRI indicates a 'corrected PRI' values calculated as the difference between PRI and PRI_o ($\Delta PRI = PRI - PRI_o$), which has been shown by others as a means of accounting for differences in constitutive pigment pools among leaves, thereby isolating the influence of facultative pigment pools on PRI (Gamon and Berry 2012; Magney et al., 2016).

Statistics. One-way analysis of variance (ANOVA) was used to test for overall differences between sun and shade leaves for pigment pools, pigment ratios, PRI and SR680 values. Differences were considered significant at $P \leq 0.01$. If the ANOVA showed an overall significant

effect, individual pairs of means were compared using Tukey's honestly significant difference (Tukey's HSD) criterion (Zar 1999). Linear regressions were used to determine relationships between spectral indices and bulk pigment pool sizes and ratios. Goodness of fit was evaluated based on the coefficient of simple determination (r^2) and root mean square error (RMSE) values.

RESULTS.

Photo-protective investment: Spectral determination of constitutive pigment pools. Sun leaves had xanthophyll cycle pigment pools (V+A+Z) more than double that of shade leaves (p=0), 30% higher bulk car (p=0), 15% higher Chl*a*+*b* (P<0.001), and 37% greater lutein (p=0). There were no statistical differences between sun and shade leaves in either zeaxanthin or beta-carotene (Fig. 1a). Similarly, the following bulk pigment ratios were significantly greater in sun compared to shade leaves: (V+A+Z)/(Chl*a*+*b*) (57% higher, p<0.001), Chl*a*/*b* (17% higher, p=0), and (bulk car)/(Chl*a* +*b*) (19% higher, p<0.01) (Fig. 1b). There was no statistically significant difference in sun compared to shade leaves in lutein/(Chl*a*+*b*) (Fig. 1b). PRI_o was more than twice as low for sun compared to shade leaves (p<0.01) (Fig. 1c), while SR680 was 30% higher in sun compared to shade leaves (p=0) (Fig. 1d).

There were moderately strong linear relationships ($r^2 \geq 0.5$, $p \leq 0.05$) between several of the spectral indices and differences in bulk pigment pools and ratios (Table 2). Only the relationships between (V+A+Z) and each of PRI_o (Fig. 2a), SR680 (Fig. 2b) and ND705 (Table 2) had regression coefficients > 0.5 ($p \leq 0.05$) (Table 2). Each of SR680, SR705, mSR705, ND680, ND705, mND705, (chl)RI_{green}, and (chl)$RI_{red\ edge}$ were related to both bulk car and lutein (Table 2, Fig. 2b,d). The (chl)RI_{red} and ND705 were the only indices that had statistically significant relationships with Chl*a*+*b*, while only MCARI was related to beta-carotene (Table 2).

Both the PRI_o and SR680 were related to Chl*a*/*b* (Table 2, Fig. 2a,c). PRI_o was more strongly related to Chl*a*/*b* than to (V+A+Z), bulk car, or bulk car/Chl*a*+*b* (Table 2). Only SR680 (Fig. 2d) and ND680 were related to (V+A+Z)/(Chl*a*+*b*) (Table 2). SR680 was the spectral vegetation index with the greatest number of moderately strong relationships with pigment pools and ratios (Table 2, Fig. 2b-d).

Photo-protective activity: Spectral determination of adjustments in facultative pigment pools. There was no statistically significant difference in dEPS between sun and shade leaves. While PRI was statistically significantly lower for sun (PRI= -0.027) compared to shade (PRI= 0.01) leaves ($p=0.003$), there were no statistically significant differences in ΔPRI. When sun and shade leaves were combined, ΔPRI was more strongly related to variation in dEPS ($r^2=0.78$, RMSE=0.01, $p<0.05$) than was PRI ($r^2=0.34$, RMSE=0.02, $p<0.05$) (Fig. 3).

DISCUSSION.

PRI as a rapid measure of both constitutive and facultative photoprotection. In agreement with our first two hypotheses, we found that PRI_o was significantly lower in sun compared to shade leaves of *Salix pulchra.* These differences appear to be at least partially driven by the differences in total xanthophyll cycle pool size reported in Magney et al. (*in review*) – since sun leaves exhibited greater investment in photoprotective mechanisms (i.e. xanthophyll cycle pool size) relative to shade leaves - but are likely also explained by co-variation among pigment variables. Our findings differ from those of a similar leaf level study conducted on two temperate coniferous species by Gamon and Berry (2012) in which dark-acclimated PRI was strongly related to differences between sun and shade leaves due to differences in their bulk chlorophyll to carotenoid pool ratios, but not to variation in xanthophyll cycle pool size (i.e. ratio of total

297 chlorophyll to (V+A+Z)). Actinic light sources were used to determine PRI on dark-acclimated
298 leaves (PRI_o) in all of these studies because while non-actinic sources at 532 nm are available,
299 those at 570 nm are not - this may be limiting our ability to determine the primary bio-chemical
300 and physical drivers of variation in PRI_o. We also found that PRI_o was correlated with Chl*a*/*b*,
301 which is a good indicator of a leaf's light history (Thayer and Bjorkman 1990, Dale and Causton
302 1992, Logan et al. 1996). However, there is no easily explained physical basis for PRI_o to be
303 sensitive to Chl*a*/*b* since the difference in absorption of photosynthetically active radiation at 531
304 nm and 570 nm (the two PRI wavelengths) is very small for both Chl*a* and Chl*b* (Lichtenthaler
305 1987). Rather, Chl*a*/*b* may distinguish between sun and shade leaves similarly to xanthophyll
306 pool size and is therefore correlated with variation in PRI_o.

307 Similar to a handful of recent temperate and boreal studies (Gamon and Berry 2012, Liu
308 et al. 2013, Hmimina et al. 2014,2015, Wong et al. 2015b, Magney et al. 2016), we were able to
309 quantitatively account for constitutive pigment pools by subtracting the dark-acclimated PRI
310 (PRI_o) from the PRI of illuminated leaves (PRI) to isolate the influence of xanthophyll cycle
311 epoxidation state on PRI. Relative to the uncorrected PRI, the corrected PRI (ΔPRI) was much
312 more strongly related to the change in xanthophyll cycle de-epoxidation that occurred during the
313 dark to light transition. As such, our Arctic-specific findings support a growing suite of studies
314 conducted at both the leaf and stand-levels in a wide variety of ecosystems and settings, showing
315 that *both* variation in chlorophyll and carotenoid pigment pools, and xanthophyll cycle activity,
316 greatly influence PRI dynamics (as reviewed in Garbulsky et al. 2011). Most recently, Wong
317 and Gamon (2015b) found that canopy level PRI was more strongly related to seasonally
318 changing carotenoid to chlorophyll ratios than to xanthophyll cycle activity in two boreal conifer
319 species (*Pinus contorta* and *Pinus ponderosa*). In a related study on the same species, Wong and

Gamon (2015a) found that the PRI and seasonal dynamics in pigment pools were closely timed with variation in several physiologic variables, including xanthophyll cycle conversion state, showing that PRI was a clear optical indicator of the onset of spring photosynthetic activation. In a study where different time scales in PRI variation were considered in both conifers and broad leaf tree species, both Porcar-Castell et al. (2012) and Gamon et al. (2015) found that while carotenoid to chlorophyll ratios did indeed have the strongest influence on canopy level PRI over the course of the spring season, diurnal variation in PRI was most affected by xanthophyll cycle activity. Similarly, other recent studies conducted at a range of spatial and temporal scales have found that PRI varies with both bulk pigment contents and xanthophyll cycle activity depending on the temporal scale being examined, and include a range of growth-forms including eggplant (Rahimzadeh-Bajgiran et al. 2012), temperate deciduous tree species (Garrity et al. 2011, Hmimina et al. 2014,2015), and wheat fields (Magney et al., 2016). Differences in PRI-pigment pool relationships among studies, including the current study, are likely due to differences in study species, spatial and temporal scales being examined, instrument specifications (Harris et al. 2014), and processing of spectral reflectance data done prior to calculation of PRI.

SR680 and other indices as rapid measures of constitutive pigment investment. We found moderately strong linear relationships between several of the indices and differences in bulk pigment pools between sun and shade leaves. These findings agree with our third hypothesis and suggest additional spectral information to that offered by the dark-acclimated PRI (PRI_o) may help estimate parameters related to resource partitioning in the form of relative pigment investments. Of the twelve vegetation indices we examined (including PRI_o) the SR680 was most suited to estimating dynamics in photoprotective investment among leaves within *Salix*

343 *pulchra* canopies. Our finding that the SR680 is correlated not only with variation in total
344 xanthophyll cycle pool size, but also with lutein pool size is particularly interesting given recent
345 evidence that the lutein epoxide cycle (Bungard et al. 1999) may also be involved in energy
346 dissipation (Garcia-Plazaola et al. 2002, 2007, Matsubara et al. 2007, Jahns and Holzwarth
347 2012). It should also be noted that several other indices we investigated were equally related to
348 both bulk carotenoids and lutein, suggesting that relative to other carotenoids, lutein may
349 contribute more significantly to spectral reflectance and/or be most strongly correlated with
350 variation in bulk carotenoid pools. However, the effect of lutein on reflectance spectra and
351 vegetation indices has only begun to be explored (Gamon and Berry 2012). In the only study we
352 know of examining these relationships, Wong et al. (2015a) found that seasonal shifts in both
353 bulk xanthophyll cycle and lutein concentrations mirrored those of PRI in two boreal pine
354 species. Further studies focused on gaining mechanistic understanding of the relationships found
355 between vegetation indices and lutein are required.
356 Due to chlorophyll's absorption spectrum, SR680 is typically employed as a 'chlorophyll
357 index', yet we found that individual and bulk carotenoid concentrations explained more of the
358 variance in SR680 (r^2= 0.62 – 0.71) than did bulk chlorophyll concentration (r^2=0.39). Since
359 carotenoids do not absorb light at 680 nm (nor at the 800 nm reference wavelength), it is likely
360 this correlation is secondary in nature since sun leaves had both higher chlorophyll and
361 carotenoid pools relative to shade leaves (see Fig. 1a). The SR680 was also correlated with
362 Chl*a*/*b*, which may be due to the fact that chlorophyll *a* absorbs more strongly than chlorophyll *b*
363 at 680 nm (Lichtenthaler 1987). We therefore suggest that the SR680 - which has an advantage
364 over PRI in that it can be employed equally well on dark-acclimated and illuminated leaves -

could be used as a rapid means of assessing resource (pigment) partitioning within arctic shrub canopies.

Of the other indices explored, ND680 performed similarly to SR680. The SR680 (R_{800}/R_{680}) is a simple ratio designed to enhance the absorption feature of the denominator wavelength relative to the numerator wavelength, while the ND680 ($R6_{800}$-R_{680}/R_{800}+R_{680}) is a normalized difference index designed to enhance the contrast of lower ratio values (Schowengerdt 2007) - both were designed to maximize pigment differences at whole canopy scales. Regardless of their different designs, the two indices performed very similarly in our leaf level study likely due the fact that they rely on the same wavelength sensitivities - 680 nm and 800 nm. The remaining vegetation indices either did not correlate with as many, or any, pigment variables. Similar to SR680 and ND680, the majority of the remaining 'chlorophyll indices' (SR705, mSR705, ND705, (chl)RI_{green}), were moderately correlated with bulk carotenoid contents (r^2 = 0.53 - 0.62) but not with bulk chlorophyll content nor Chl*a*/*b*. We suggest that the SR705, mSR705 and ND705 were not as strongly related to Chl*a*/*b* relative to the 680 nm indices because chlorophyll *a* and *b* both absorb equally weakly at 705 nm, whereas at 680 nm chlorophyll *a* is a much stronger absorber than chlorophyll *b* (Lichtenthaler 1987). Further, the fact that none of the 705 nm indices were correlated with either bulk xanthophyll pools or Chl*a*/*b*, while the 680 nm indices were correlated with both, highlights the secondary nature of the relationship between SR680 (and ND680) and bulk xanthophyll pools – in other words, SR680 and ND680 are influenced directly by variation in Chl*a*/*b* which likely co-varies with xanthophyll pool size among shade and sun leaves. The MCARI was the only index correlated with the carotenoid beta-carotene which has an absorption range at wavelengths shorter than any of those used in the MCARI (Vetter et al. 1971), suggesting that this relationship is likely

388 secondary in nature. We suggest that several of the vegetation indices we explored did not
389 correlate well with pigment pools for two main reasons: (1) our study leaves had relatively small
390 inter-leaf variation in chlorophyll and carotenoid contents, and therefore little difference among
391 spectral absorption features in the visible wavelengths and; (2) several of the indices explored
392 were designed as canopy level indices and may not be well-suited for leaf level studies such as
393 ours. Nevertheless, our findings are unique because while many previous studies have shown
394 that several of the same vegetation indices explored often vary closely with relatively large
395 changes in leaf pigment pools associated with seasonality or along environmental gradients
396 (Rahman et al. 2001, Sims and Gamon 2002, Whitehead et al. 2005, Martin and Asner 2009,
397 Gamon et al. 2012,2015, Soudani et al. 2014), we show that select indices were sensitive to a
398 much smaller range in pigment pool dynamics that occur within arctic shrub canopies during the
399 period of maximum canopy greenness. This is particularly useful as it allows rapid spectral
400 assessment of the resource partitioning recently discovered in arctic shrub canopies (Magney et
401 al., *in press*).

402 Finally, an important caveat to our study is that because it was conducted during the
403 period of maximum leaf out, the findings and relationships presented here may not hold through
404 an entire Arctic growing season since leaf internal structure and biochemical composition, as
405 well as leaf surface properties, change in ways that likely have differential effects on spectral
406 reflectance characteristics (Jacquemoud and Baret 1990, Carter and Knapp 1991, Penuelas et al.
407 1995, Sims and Gamon 2002, Merzlyak et al. 2003, Levizou et al. 2005). We therefore suggest
408 that future work build on the pigment-spectral relationships presented herein by exploring
409 relationships between the various vegetation indices and pigment pools over the course of an
410 entire Arctic growing season, and expand upon the current study by including additional

411 deciduous shrub species that are becoming increasingly dominant in our study region (ie. other
412 willow species, dwarf birch, and alder species). Given the seasonal (climatic) and structural
413 (vegetative) changes that are occurring in the Arctic, this topic is prime for further study.

414 **Implications.** Our findings contribute insight and practical techniques for using leaf level
415 spectral vegetation indices as rapid, non-destructive and repeatable estimates of rapid facultative
416 dynamics in leaf-level xanthophyll activity (using ΔPRI) and more sustained differences in
417 constitutive pigment pools (using SR680) - and potentially light use efficiency - within tall
418 deciduous shrub canopies in the Arctic. To our knowledge, this is the only Arctic-specific
419 information related to the use of PRI (Garbulsky et al. 2011) or any other spectral index to study
420 within canopy resource partitioning in Arctic tundra. This is timely given: (1) tall deciduous
421 shrubs are rapidly increasing in height, density, and range in many Arctic regions at the expense
422 of low-lying graminoid communities (Myers-Smith et al. 2011) and this trend is projected to
423 continue into the future (Pearson et al. 2013), (2) the recent findings that deciduous shrubs are
424 already exhibiting within canopy resource partitioning as function of within canopy gradients in
425 light availability (Magney et al. *in press*) suggesting that light use efficiency will become an
426 increasingly important variable to include in modeling tundra NEE in the future, and, (3) the
427 widely used canopy level NDVI - used in calculating GPP and ER used in modeling tundra NEE
428 (Shaver et al. 2007) - when employed alone, is insensitive to dynamics in light use efficiency
429 (Gamon et al. 1995, Asner et al. 2004). Our findings do not directly advance the employment of
430 space-based PRI measurements to quantify spatial variation in tundra photosynthesis because
431 disentangling the relative influence of constitutive and facultative pigment pools on PRI requires
432 dark acclimation of foliage. However, similar to Magney et al. (2016), it may be worth exploring
433 if a PRI measurement taken during low irradiance (ie. when the sun is very near the horizon

434 during arctic summer nights) could be subtracted from a PRI measurement collected during light
435 saturation from satellite instruments with overpass times separated by more than a few hours –
436 though such data is not readily available. Instead, we suggest future work explore relationships
437 between canopy level spectra and within canopy variation in leaf level PRI and SR680 so that
438 both long- and short-term dynamics in the efficiency with which incident light is absorbed and
439 converted to fixed carbon can be better incorporated into tundra NEE models.

440

441 **ACKNOWLEDGEMENTS.** This work was supported by NASA Terrestrial Ecology grant
442 NNX12AK83G. We thank Toolik Field Station (Institute of Arctic Biology, University of Alaska
443 Fairbanks) and the Arctic LTER for support and logistics. We thank Shannan Sweet for her
444 assistance with data analysis.

445

446 **REFERENCES.**

447 Asner GP, Nepstad D, Cardinot G, Ray D. 2004. Drought stress and carbon uptake in an Amazon
448 forest measured with spaceborne imaging spectroscopy. Proceedings of the National Academy of
449 Sciences of the United States of America 101: 6039–6044.
450 Bilger W., Björkman O., Thayer S.S. (1989) Light-induced spectral absorbance changes in
451 relation to photosynthesis and the epoxidation state of xanthophyll cycle components in cotton
452 leaves. Plant Physiol. 91:542-551
453 Blackburn GA. 2007. Hyperspectral remote sensing of plant pigments. Journal of Experimental
454 Botany 58: 855–867.

455 Boelman NT, Gough L, McLaren JR, Greaves H. 2011. Does NDVI reflect variation in the
456 structural attributes associated with increasing shrub dominance in arctic tundra? Environmental
457 Research Letters 6: 035501.
458 Bréda NJJ. 2003. Ground-based measurements of leaf area index: A review of methods,
459 instruments and current controversies. Journal of Experimental Botany 54: 2403–2417.
460 Bungard RA, Ruban A V, Hibberd JM, Press MC, Horton P, Scholes JD. 1999. Unusual
461 carotenoid composition and a new type of xanthophyll cycle in plants. Proceedings of the
462 National Academy of Sciences of the United States of America 96: 1135–1139.
463 Butler WL. 1978. Energy distribution in the photochemical apparatus of photosynthesis. Annual
464 Review of Plant Physiology 29: 345–378.
465 Caldwell MM. 1981. Plant Response to Solar Ultraviolet Radiation. In: Lange et al., OL, ed.
466 Physiological Plant Ecology I. Heidelberg: Springer-Verlag Berlin, 169–197.
467 Carter GA, Knapp AK. 2001. Leaf optical properties in higher plants: linking spectral
468 characteristics to stress and chlorophyll concentration. American journal of botany 88: 677–684.
469 Dale MP, Causton DR. 1992. The ecophysiology of Veronica V . montana IV . Effects of
470 shading on nutrient allocations - a field experiment. Journal of Ecology 80: 517–526.
471 Daughtry C, Walthall C, Kim M, De Colstoun EB, McMurtreyIII J. 2000. Estimating corn leaf
472 chlorophyll concentration from leaf and canopy reflectance. Remote Sensing of Environment 74:
473 229–239.
474 Demmig-Adams B. 1998. Survey of Thermal Energy Dissipation and Pigment Composition in
475 Sun and Shade Leaves. Plant and Cell Physiology 39: 474–482.
476 Demmig-Adams B, Adams WW. 1996. The role of xanthophyll cycle carotenoids in the
477 protection of photosynthesis. Trends in Plant Science 1: 21–26.

478 Demmig-Adams B, Adams III WW. 1992. Responses of Plants To High Light Stress. Annual
479 Review of Plant Physiology 43: 599–626.
480 Field, CB. 1991. Ecological scaling of carbon gain to stress and resource availability. In:
481 Mooney HA, Winner WE, Pell EJ, eds. Response of plants to multiple stresses. New York, USA:
482 Academic Press, 35-65.

483 Filella I, Amaro T, Araus JL, Peñuelas J. 1996. Relationship between photosynthetic radiation-
484 use efficiency of barley canopies and the photochemical reflectance index (PRI). Physiologia
485 Plantarum 96: 211–216.
486 Fraser RH, Olthof I, Carrière M, Deschamps A, Pouliot D. 2011. Detecting long-term changes to
487 vegetation in northern Canada using the Landsat satellite image archive. Environmental Research
488 Letters 6: 045502.
489 Gamon JA, Berry JA. 2012. Facultative and constitutive pigment effects on the Photochemical
490 Reflectance Index (PRI) in sun and shade conifer needles. Israel Journal of Plant Sciences 60:
491 85–95.
492 Gamon JA, Field CB, Goulden ML, Griffin KL, Anne E, Joel G, Peñuelas J, Valentini R. 1995.
493 Relationships between NDVI, canopy structure, and photosynthesis in three Californian
494 vegetation types. Ecological Applications 5: 28–41.
495 Gamon JA, Kovalchuk O, Wong CYS, Harris A, Garrity SR. 2015. Monitoring seasonal and
496 diurnal changes in photosynthetic pigments with automated PRI and NDVI sensors.
497 Biogeosciences Discussions 12: 2947–2978.
498 Garbulsky MF, Peñuelas J, Gamon J, Inoue Y, Filella I. 2011. The photochemical reflectance
499 index (PRI) and the remote sensing of leaf, canopy and ecosystem radiation use efficiencies. A
500 review and meta-analysis. Remote Sensing of Environment 115: 281–297.

501 Gamon JA, Qiu HL. 1999. Ecological applications of remote sensing at multiple scales. pp. 805-
502 846 In: Pugnaire FI, Valladares F (Eds) Handbook of Functional Plant Ecology. Marcel Dekker,
503 Inc. New York.
504 Garcia-Plazaola JI, Hernandez A, Errasti E, Becerril JM. 2002. Occurrence and operation of the
505 lutein epoxide cycle in Quercus species. Functional Plant Biology 29: 1075–1080.
506 García-Plazaola JI, Matsubara S, Osmond CB. 2007. The lutein epoxide cycle in higher plants:
507 Its relationships to other xanthophyll cycles and possible functions. Functional Plant Biology 34:
508 759–773.
509 Garrity SR, Eitel JUH, Vierling LA. 2011. Disentangling the relationships between plant
510 pigments and the photochemical reflectance index reveals a new approach for remote estimation
511 of carotenoid content. Remote Sensing of Environment 115: 628–635.
512 Gilmore AM, Yamamoto HY. 1991. Resolution of lutein and zeaxanthin using a non-endcapped,
513 lightly carbon-loaded C18 high-performance liquid chromatographic column. Journal of
514 Chromatography A 543: 137–145.
515 Gilmore AM, Yamamoto HY. 1993. Linear models relating xanthophylls and lumen acidity to
516 non-photochemical fluorescence quenching. Evidence that antheraxanthin explains zeaxanthin-
517 independent quenching. Photosynthesis Research 35: 67–78.
518 Gitelson A a., Viña A, Verma SB, Rundquist DC, Arkebauer TJ, Keydan G, Leavitt B, Ciganda
519 V, Burba GG, Suyker AE. 2006. Relationship between gross primary production and chlorophyll
520 content in crops: Implications for the synoptic monitoring of vegetation productivity. Journal of
521 Geophysical Research: Atmospheres 111: 1–13.

522 Hall FG, Hilker T, Coops NC, Lyapustin A, Huemmrich KF, Middleton E, Margolis H, Drolet
523 G, Black TA. 2008. Multi-angle remote sensing of forest light use efficiency by observing PRI
524 variation with canopy shadow fraction. Remote Sensing of Environment 112: 3201–3211.
525 Harris, A., J. A. Gamon, G. Z. Pastorello, and C. Y. S. Wong. 2014. Retrieval of the
526 photochemical reflectance index for assessing xanthophyll cycle activity: a comparison of near-
527 surface optical sensors. Biogeosciences 11:6277–6292.
528 Hartel H, Lokstein H, Grimm B, Rank B. 1996. Kinetic Studies on t e Xanthophyll Cycle in
529 Barley Leaves '. Plant physiology 110: 471–482.
530 Hmimina G, Dufrêne E, Soudani K. 2014. Relationship between photochemical reflectance
531 index and leaf ecophysiological and biochemical parameters under two different water statuses:
532 Towards a rapid and efficient correction method using real-time measurements. Plant, Cell and
533 Environment 37: 473–487.
534 Hmimina G, Merlier E, Dufrêne E, Soudani K. 2015. Deconvolution of pigment and
535 physiologically related photochemical reflectance index variability at the canopy scale over an
536 entire growing season. Plant, Cell & Environment 38: 1578–1590.
537 Jacquemoud S, Baret F. 1990. PROSPECT: A model of leaf optical properties spectra. Remote
538 Sensing of Environment 34: 75–91.
539 Jahns P, Holzwarth AR. 2012. The role of the xanthophyll cycle and of lutein in photoprotection
540 of photosystem II. Biochimica et Biophysica Acta - Bioenergetics 1817: 182–193.
541 Levizou, E., Drilias, P., Psaras, G. K. and Manetas, Y. (2005), Nondestructive assessment of leaf
542 chemistry and physiology through spectral reflectance measurements may be misleading when changes
543 in trichome density co-occur. New Phytologist, 165: 463-472. doi: 10.1111/j.1469-8137.2004.01250.x

544 Lichtenthaler HK. 1987. Chlorophylls and carotenoids: Pigments of photosynthetic
545 biomembranes. Methods in Enzymology. ACADEMIC PRESS, INC., 350–382.
546 Liu L, Zhang Y, Jiao Q, Peng D. 2013. Assessing photosynthetic light-use efficiency using a
547 solar-induced chlorophyll fluorescence and photochemical reflectance index. International
548 Journal of Remote Sensing 34: 4264–4280.
549 Logan BA, Barker DH, Demmig Adams B, Adams III WW. 1996. Acclimation of leaf
550 carotenoid composition and ascorbate levels to gradients in the light environment within an
551 Australian rainforest. Plant Cell and Environment 19: 1083–1090.
552 Loranty MM, Goetz SJ. 2012. Shrub expansion and climate feedbacks in Arctic tundra.
553 Environmental Research Letters 7: 011005.
554 Macias-Fauria M, Forbes BC, Zetterberg P, Kumpula T. 2012. Eurasian Arctic greening reveals
555 teleconnections and the potential for structurally novel ecosystems. Nature Climate Change 2:
556 613–618.
557 Magney TS, Eitel JUH, Griffin KL, Boelman NT, Logan NB, Zheng G, Greaves H, Prager C,
558 Oliver R, Fortin L, Ma L, Vierling LA. *in press.* LiDAR derived canopy model reveals patterns
559 of photosynthetic partitioning in an arctic shrub. Agricultural and Forest Meteorology.
560 Magney TS, Logan BA, Griffin KL, Reblin J, Abatzoglou J, Eitel JUH, Boelman NT, Greaves
561 H, Prager C, Vierling LA. *In review.* The response of xanthophyll mediated photoprotection to
562 climate: a meta-analysis of higher plant species. *Global Ecology and Biogeography*.
563 Magney, TS, Vierling, LA, Eitel, JUH, Huggins, DR, & Garrity, SR (2016). Response of high
564 frequency Photochemical Reflectance Index (PRI) measurements to environmental conditions in
565 wheat. *Remote Sensing of Environment*, *173*, 84–97. http://doi.org/10.1016/j.rse.2015.11.013

566 Martin RE, Asner GP. 2009. Leaf chemical and optical properties of metrosideros polymorpha
567 across environmental gradients in Hawaii. Biotropica 41: 292–301.
568 Matsubara S, Morosinotto T, Osmond CB, Bassi R. 2007. Short- and long-term operation of the
569 lutein-epoxide cycle in light-harvesting antenna complexes. Plant physiology 144: 926–941.
570 McGuire AD, Anderson LG, Christensen TR, Dallimore S, Guo LD, Hayes DJ, Heimann M,
571 Lorenson TD, Macdonald RW, Roulet N. 2009. Sensitivity of the carbon cycle in the Arctic to
572 climate change. Ecological Monographs 79: 523–555.
573 McManus KM, Morton DC, Masek JG, Wang D, Sexton JO, Nagol JR, Ropars P, Boudreau S.
574 2012. Satellite-based evidence for shrub and graminoid tundra expansion in northern Quebec
575 from 1986 to 2010. Global Change Biology 18: 2313–2323.
576 Merzlyak MN, Gitelson AA, Chivkunova OB, Solovchenko AE, Pogosyan SI. 2003. Application
577 of reflectance spectroscopy for analysis of higher plant pigments. Plant Physiol. 50: 704–710.
578 Myers-Smith IH, Elmendorf SC, Beck PSA, Wilmking M, Hallinger M, Blok D, Tape KD,
579 Rayback SA, Macias-Fauria M, Forbes BC, et al. 2015. Climate sensitivity of shrub growth
580 across the tundra biome. Nature Climate Change.
581 Nakaji T, Oguma H, Fujinuma Y. 2006. Seasonal changes in the relationship between
582 photochemical reflectance index and photosynthetic light use efficiency of Japanese larch
583 needles. International Journal of Remote Sensing 27: 493–509.
584 Niinemets Ü. 2010. A review of light interception in plant stands from leaf to canopy in different
585 plant functional types and in species with varying shade tolerance. Ecological Research 25: 693–
586 714.

587 Niinemets Ü, Bilger W, Kull O, Tenhunen JD. 1998. Acclimation to high irradiance in temperate
588 deciduous trees in the field: Changes in xanthophyll cycle pool size and in photosynthetic
589 capacity along a canopy light gradient. Plant, Cell and Environment 21: 1205–1218.
590 Niinemets Ü, Bilger W, Kull O, Tenhunen J. 1999. Responses of foliar photosynthetic electron
591 transport, pigment stoichiometry, and stomatal conductance to interacting environmental factors
592 in a mixed species forest canopy. Tree physiology 19: 839–852.
593 Peguero-Pina JJ, Gil-Pelegrín E, Morales F. 2013. Three pools of zeaxanthin in Quercus
594 coccifera leaves during light transitions with different roles in rapidly reversible photoprotective
595 energy dissipation and photoprotection. Journal of Experimental Botany 64: 1649–1661.
596 Peñuelas J. 2011. Letters Photochemical reflectance index (PRI) and remote sensing of plant
597 CO uptake. New Phytologist 191: 596–599.
598 Penuelas J, Baret F, Filella I. 1995. Semiempirical Indexes to Assess Carotenoids Chlorophyll-a
599 Ratio from Leaf Spectral Reflectance. Photosynthetica 31: 221–230.
600 Porcar-Castell A, Garcia-Plazaola JI, Nichol CJ, Kolari P, Olascoaga B, Kuusinen N, Fernández-
601 Marín B, Pulkkinen M, Juurola E, Nikinmaa E. 2012. Physiology of the seasonal relationship
602 between the photochemical reflectance index and photosynthetic light use efficiency. Oecologia
603 170: 313–323.
604 Powles SB. 1984. Photoinhibition of Photosynthesis Induced by Visible Light. Annual Review
605 of Plant Physiology 35: 15–44.
606 Rahimzadeh-Bajgiran P, Munehiro M, Omasa K. 2012. Relationships between the
607 photochemical reflectance index (PRI) and chlorophyll fluorescence parameters and plant
608 pigment indices at different leaf growth stages. Photosynthesis Research 113: 261–271.

609 Rahman AF, Gamon JA, Fuentes DA, Roberts DA, Prentiss D. 2001. Modeling spatially
610 distributed ecosystem flux of boreal forest using hyperspectral indices from AVIRIS imagery.
611 Journal of Geophysical Research 106: 33579.
612 Schowengerdt RA. 2007. Remote sensing models and methods for image processing. New York,
613 USA: Academic Press.
614 Sims D, Gamon JA. 2002. Relationships between leaf pigment content and spectral reflectance
615 across a wide range of species, leaf structures and developmental stages. Remote Sensing of
616 Environment 81: 337–354.
617 Sims DA, Luo H, Hastings S, Oechel WC, Rahman AF, Gamon JA. 2006. Parallel adjustments
618 in vegetation greenness and ecosystem CO2 exchange in response to drought in a Southern
619 California chaparral ecosystem. Remote Sensing of Environment 103: 289–303.
620 Soudani K, Hmimina G, Dufrêne E, Berveiller D, Delpierre N, Ourcival JM, Rambal S, Joffre R.
621 2014. Relationships between photochemical reflectance index and light-use efficiency in
622 deciduous and evergreen broadleaf forests. Remote Sensing of Environment 144: 73–84.
623 Sweet SK, Griffin KL, Steltzer H, Gough L, Boelman NT. 2014. Greater deciduous shrub
624 abundance extends tundra peak season and increases modeled net CO 2 uptake. Global Change
625 Biology: n/a–n/a.
626 Thayer SS, Björkman O. 1990. Leaf Xanthophyll content and composition in sun and shade
627 determined by HPLC. Photosynthesis Research 23: 331–343.
628 Ustin SL, Gitelson AA, Jacquemoud S, Schaepman M, Asner GP, Gamon JA, Zarco-Tejada P.
629 2009. Retrieval of foliar information about plant pigment systems from high resolution
630 spectroscopy. Remote Sensing of Environment 113.

631 Vetter W, Englert G, Rigassi N, Schwieter U. 1971. Spectroscopic Methods. In: Isler O,
632 Gutmann H, Solms U, eds. Carotenoids. Basel, Switzerland: Springer Basel, 189-266.
633 Walker MD, Wahren CH, Hollister RD, Henry GHR, Ahlquist LE, Alatalo JM, Bret-Harte MS,
634 Calef MP, Callaghan T V, Carroll AB, et al. 2006. Plant community responses to experimental
635 warming across the tundra biome. Proceedings of the National Academy of Sciences of the
636 United States of America 103: 1342–1346.
637 Whitehead D, Boelman NT, Turnbull MH, Griffin KL, Tissue DT, Barbour MM, Hunt JE,
638 Richardson SJ, Peltzer DA. 2005. Photosynthesis and reflectance indices for rainforest species in
639 ecosystems undergoing progression and retrogression along a soil fertility chronosequence in
640 New Zealand. Oecologia 144: 233–244.
641 Williams M, Bell R, Spadavecchia L, Street LE, Van Wijk MT. 2008. Upscaling leaf area index
642 in an Arctic landscape through multiscale observations. Global Change Biology 14: 1517–1530.
643 Williams M, Rastetter EB. 1999. Vegetation characteristics and primary productivity along an
644 arctic transect: implications for scaling-up. Journal of Ecology 87: 885–898.
645 Williams M, Rastetter EB, Shaver GR, Hobbie JE, Carpino E, Kwiatkowski BL. 2001. Primary
646 production of an arctic watershed: An uncertainty analysis. Ecological Applications 11: 1800–
647 1816.
648 Wong CYS, Gamon JA. 2015a. The photochemical reflectance index provides an optical
649 indicator of spring photosynthetic activation in evergreen conifers. New Phytologist 206: 196–
650 208.
651 Wong CYS, Gamon JA. 2015b. Three causes of variation in the photochemical reflectance index
652 (PRI) in evergreen conifers. New Phytologist 206: 187–195.
653

TABLES.

Table 1. Various spectral vegetation indices used in this study that have been previously shown to be related to foliar pigment (chlorophylls and carotenoids) concentrations.

Name	Type[a]	Abbreviation	Equation[b]	References
Photochemical reflectance index	carotenoids	PRI	$(R_{531}-R_{570})/(R_{531}+R_{570})$	Gamon, Penuleas and Field et al. 1993
Structure Intensive Pigment Index	carotenoids	SIPI	$(R_{800} - R_{445})/ (R_{800} + R_{680})$	Penuelas et al. 1995
Plant Senescence Reflectance Index	carotenoids	PSRI	$(R_{680} - R_{500})/R_{750}$	Merzlyak et al. 1999
Simple ratio 680 nm	chlorophylls	SR680	R_{800}/R_{680}	Berth and McVey 1968, Sims and Gamon 2002
Simple ratio 705 nm	chlorophylls	SR705	R_{750}/R_{705}	Gitelson and Merzlyak 1994, Sims and Gamon 2002
Modified simple ratio 705 nm	chlorophylls	mSR705	$(R_{750} - R_{445})/ (R_{750} + R_{445})$	Sims and Gamon 2002
Normalized difference 680 nm	chlorophylls	ND680 (or $NDVI_{680}$)	$(R_{800} - R_{680})/ (R_{800} + R_{680})$	Berth and McVey 1968, Sims and Gamon 2002
Normalized difference 705 nm	chlorophylls	ND705 (or $NDVI_{705}$)	$(R_{750} - R_{705})/ (R_{750} + R_{705})$	Gitelson and Merzlyak 1994, Sims and Gamon 2002
Modified normalized difference 705 nm	chlorophylls	mND705	$(R_{750} - R_{705})/ (R_{750} + R_{705} - 2R_{445})$	Sims and Gamon 2002
Chlorophyll reflectance index green	chlorophylls	$(Chl)RI_{green}$	$(R_{750\text{-}800} - R_{520\text{-}585}) - 1$	Gitelson and Merzlyak 2004
Chlorophyll reflectance index red edge	chlorophylls	$(Chl)RI_{red\ edge}$	$(R_{750\text{-}800} - R_{695\text{-}740}) - 1$	Gitelson and Merzlyak 2004
Modified chlorophyll absorption index	chlorophylls	MCARI	$[(R_{700}- R_{670}) - 0.2 * (R_{700}- R_{550})] * (R_{700}/ R_{670})$	Daughtry et al. 2000

[a] Indices are grouped based on the pigment group (carotenoids or chlorophylls) they were each designed to be sensitive to.

[b] $R_{###}$ indicates the reflectance value at a specific wavelength or range of wavelengths (in nanonmeters, nm) used to calculate each index.

Table 2. Correlation coefficient (r^2, top value) and root mean square error (RMSE, bottom italicized value) values for relationships between various spectral vegetation indices and constitutive bulk pigment pool sizes and ratios. Bold text indicates r^2 values > 0.5 with $p \leq 0.05$.

	Spectral Vegetation Indices											
Pigment pool size or ratio	PRI_o	SIPI	PSRI	SR680	SR705	mSR705	ND680	ND705	mND705	$(chl)RI_{green}$	$(chl)RI_{red\ edge}$	MCARI
Chl*a+b*	0.30	0.01	0.05	0.39	0.47	0.43	0.32	0.49	0.44	0.33	**0.51**	0.06
	32.70	*42.40*	*42.00*	*33.58*	*31.39*	*32.66*	*35.55*	*30.91*	*32.30*	*35.32*	*30.20*	*41.83*
(V+A+Z)	**0.59**	0.08	0.14	**0.69**	0.38	0.26	**0.67**	0.39	0.26	0.43	0.38	0.01
	11.23	*19.62*	*19.00*	*11.35*	*16.08*	*17.63*	*11.75*	*15.98*	*17.57*	*15.43*	*16.12*	*20.34*
neaxanthin	0.01	0.06	0.06	0.12	0.07	0.08	0.07	0.07	0.08	0.08	0.06	0.00
	4.88	*4.11*	*4.04*	*3.91*	*4.02*	*4.01*	*4.02*	*4.02*	*4.00*	*4.00*	*4.04*	*4.16*
lutein	0.44	0.13	0.25	**0.71**	**0.53**	0.41	**0.65**	**0.53**	0.40	**0.52**	**0.51**	0.01
	8.44	*10.58*	*10.23*	*6.42*	*8.12*	*9.07*	*6.98*	*8.10*	*9.15*	*8.18*	*8.29*	*11.78*
beta-carotene	0.01	0.04	0.00	0.01	0.31	0.42	0.01	0.34	0.46	0.22	0.38	**0.56**
	7.03	*6.81*	*7.26*	*7.22*	*6.02*	*5.51*	*7.25*	*5.88*	*5.33*	*6.42*	*5.74*	*4.84*
bulk car	0.35	0.05	0.17	**0.62**	**0.58**	**0.53**	**0.56**	**0.61**	**0.56**	**0.57**	**0.60**	0.04
	30.75	*34.71*	*36.48*	*24.74*	*25.81*	*27.42*	*26.47*	*25.14*	*26.66*	*26.10*	*25.17*	*39.20*
Chl*a/b*	**0.64**	0.13	0.11	**0.52**	0.10	0.03	0.47	0.10	0.03	0.08	0.09	0.24
	0.22	*0.36*	*0.35*	*0.26*	*0.35*	*0.36*	*0.27*	*0.35*	*0.36*	*0.36*	*0.35*	*0.32*
lutein/Chl*a* +b	0.08	0.03	0.02	0.19	0.13	0.09	0.21	0.13	0.09	0.21	0.10	0.00
	0.04	*0.04*	*0.04*	*0.04*	*0.04*	*0.04*	*0.04*	*0.04*	*0.04*	*0.04*	*0.04*	*0.04*
(V+A+Z)/Chl*a+b*	0.46	0.06	0.11	**0.52**	0.24	0.15	**0.53**	0.25	0.16	0.33	0.24	0.03
	39.33	*61.01*	*59.07*	*43.41*	*54.44*	*57.66*	*42.77*	*54.06*	*57.39*	*51.22*	*54.77*	*61.72*
bulk car/Chl*a* +b	0.15	0.03	0.06	0.33	0.23	0.17	0.33	0.24	0.18	0.33	0.21	0.00
	0.08	*0.10*	*0.10*	*0.08*	*0.09*	*0.09*	*0.08*	*0.09*	*0.09*	*0.08*	*0.09*	*0.10*

669 **FIGURE CAPTIONS.**

670 **Figure 1 a** Mean constitutive leaf pigment concentrations for sun (*gray bars*) and shade (*black bars*) leaves of *Salix pulchra*. Bulk
671 carotenoids (*bulk car/10*) (in μmol/m^2), xanthophyll cycle carotenoids (*V+A+Z*) (in μmol/m^2), total chlorophyll pool size
672 ((*Chla+b)/10* (in mmol/m^2), and individual carotenoid pool sizes (in umol/m^2): violaxanthin (*V*), antheraxanthin (*A*), zeaxanthin (*Z*),
673 neaxanthin, lutein, and beta-carotene. **b** Mean pigment ratios for sun and shade leaves: *(V+A+Z)/(Chla+b)* (in mmol/mol),
674 *(Chla/b)/10*, *lutein/(Chla+b)* (in mmol/mol), and *(bulk car)/(Chla+b)* (in mmol/mol). Note that these *(V+A+Z)/(Chla+b)* values were
675 previously reported by Magney et al. (in review). **c** Mean dark-acclimated (PRI_o) and **d** *SR680*, for sun and shade leaves. Error bars
676 represent ±1 standard error of the mean (SEM). Asterisks indicate statistically significant differences between sun and shade leaves as
677 follows: * indicates $p < 0.01$,
678 ** indicates $p< 0.001$, and *** indicates $p = 0$.

679 **Figure 2a-d** Relationships between leaf pigment pools and vegetation indices. **a** Relationships between dark-acclimated PRI (PRI_o)
680 and each of total xanthophyll pigment pool size ((*V+A+Z)*, *filled squares, solid line*) (in umol/m^2) ($y = -928.19x + 50.91$, $r^2 = 0.59$,
681 $p\leq0.05$) and *Chla/b* (*open squares, dashed line*) ($y = -19.55x + 3.42$, $r^2 = 0.64$, $p\leq0.05$). **b** Relationships between SR680 and each of
682 total xanthophyll cycle pool size ((*V+A+Z)*, *filled squares*) (in umol/m^2) ($y = 5.30x - 40.21$, $r^2 = 0.69$, $p\leq0.05$).

683

684 and lutein (*open circles*) (in umol/m^2) (y = 3.13x - 1.76, r^2 = 0.66, p≤0.05). **c** Relationships between SR680 and *Chla/b* (*open*

685 *squares*) (y = 0.08x + 1.89, r^2 = 0.52, p≤0.05). **d** Relationships between SR680 and each of bulk carotenoid pool size (*bulk car*, *filled*

686 *diamonds*) (in umol/m^2) (y = 9.78x + 17.67, r^2=0.62, p≤0.05) and *(V+A+Z)/(Chla+b)* (*open diamonds)* (in mmol/mol) (y = 14.04x -

687 93.62, r^2 = 0.52, p≤0.05). Error bars represent ±1 standard error of the mean SEM.

688 **Figure 3** Relationships between dEPS and each of PRI (*filled circles, solid line)* (y = -0.18x + 0.04, r^2 = 0.34, p≤0.05) and ΔPRI

689 (*open circles, dashed line)* (y = -0.16x + 0.02, r^2 = 0.78, p≤0.05) for sun and shade leaves combined. Error bars represent ±1 standard

690 error of the mean (SEM).

Table 1

Name	Type[a]	Abbreviation	Equation[b]	References
Photochemical reflectance index	carotenoids	PRI	$(R_{531}-R_{570})/(R_{531}+R_{570})$	Gamon, Penuleas and Field et al. 1993
Structure Intensive Pigment Index	carotenoids	SIPI	$(R_{800} - R_{445})/ (R_{800} + R_{680})$	Penuelas et al. 1995
Plant Senescence Reflectance Index	carotenoids	PSRI	$(R_{680} - R_{500})/R_{750}$	Merzlyak et al. 1999
Simple ratio 680 nm	chlorophylls	SR680	R_{800}/R_{680}	Berth and McVey 1968, Sims and Gamon 2002
Simple ratio 705 nm	chlorophylls	SR705	R_{750}/R_{705}	Gitelson and Merzlyak 1994, Sims and Gamon 2002
Modified simple ratio 705 nm	chlorophylls	mSR705	$(R_{750} - R_{445})/ (R_{750} + R_{445})$	Sims and Gamon 2002
Normalized difference 680 nm	chlorophylls	ND680 (or $NDVI_{680}$)	$(R_{800} - R_{680})/ (R_{800} + R_{680})$	Berth and McVey 1968, Sims and Gamon 2002
Normalized difference 705 nm	chlorophylls	ND705 (or $NDVI_{705}$)	$(R_{750} - R_{705})/ (R_{750} + R_{705})$	Gitelson and Merzlyak 1994, Sims and Gamon 2002
Modified normalized difference 705 nm	chlorophylls	mND705	$(R_{750} - R_{705})/ (R_{750} + R_{705} - 2R_{445})$	Sims and Gamon 2002
Chlorophyll reflectance index green	chlorophylls	$(Chl)RI_{green}$	$(R_{750-800} - R_{520-585}) - 1$	Gitelson and Merzlyak 2004
Chlorophyll reflectance index red edge	chlorophylls	$(Chl)RI_{red\ edge}$	$(R_{750-800} - R_{695-740}) - 1$	Gitelson and Merzlyak 2004
Modified chlorophyll absorption index	chlorophylls	MCARI	$[(R_{700}- R_{670}) - 0.2 * (R_{700}- R_{550})] * (R_{700}/ R_{670})$	Daughtry et al. 2000

[a] Indices are grouped based on the pigment group (carotenoids or chlorophylls) they were each designed to be sensitive to.

[b] $R_{###}$ indicates the reflectance value at a specific wavelength or range of wavelengths (in nanonmeters, nm) used to calculate each index.

Table 2

	Spectral Vegetation Indices											
Pigment pool size or ratio	PRI_o	SIPI	PSRI	SR680	SR705	mSR705	ND680	ND705	mND705	$(chl)RI_{green}$	$(chl)RI_{red\ edge}$	MCARI
Chl*a+b*	0.30	0.01	0.05	0.39	0.47	0.43	0.32	0.49	0.44	0.33	**0.51**	0.06
	32.70	*42.40*	*42.00*	*33.58*	*31.39*	*32.66*	*35.55*	*30.91*	*32.30*	*35.32*	*30.20*	*41.83*
(V+A+Z)	**0.59**	0.08	0.14	**0.69**	0.38	0.26	**0.67**	0.39	0.26	0.43	0.38	0.01
	11.23	*19.62*	*19.00*	*11.35*	*16.08*	*17.63*	*11.75*	*15.98*	*17.57*	*15.43*	*16.12*	*20.34*
neaxanthin	0.01	0.06	0.06	0.12	0.07	0.08	0.07	0.07	0.08	0.08	0.06	0.00
	4.88	*4.11*	*4.04*	*3.91*	*4.02*	*4.01*	*4.02*	*4.02*	*4.00*	*4.00*	*4.04*	*4.16*
lutein	0.44	0.13	0.25	**0.71**	**0.53**	0.41	**0.65**	**0.53**	0.40	**0.52**	**0.51**	0.01
	8.44	*10.58*	*10.23*	*6.42*	*8.12*	*9.07*	*6.98*	*8.10*	*9.15*	*8.18*	*8.29*	*11.78*
beta-carotene	0.01	0.04	0.00	0.01	0.31	0.42	0.01	0.34	0.46	0.22	0.38	**0.56**
	7.03	*6.81*	*7.26*	*7.22*	*6.02*	*5.51*	*7.25*	*5.88*	*5.33*	*6.42*	*5.74*	*4.84*
bulk car	0.35	0.05	0.17	**0.62**	**0.58**	**0.53**	**0.56**	**0.61**	**0.56**	**0.57**	**0.60**	0.04
	30.75	*34.71*	*36.48*	*24.74*	*25.81*	*27.42*	*26.47*	*25.14*	*26.66*	*26.10*	*25.17*	*39.20*
Chl*a/b*	**0.64**	0.13	0.11	**0.52**	0.10	0.03	0.47	0.10	0.03	0.08	0.09	0.24
	0.22	*0.36*	*0.35*	*0.26*	*0.35*	*0.36*	*0.27*	*0.35*	*0.36*	*0.36*	*0.35*	*0.32*
lutein/Chl*a* +b	0.08	0.03	0.02	0.19	0.13	0.09	0.21	0.13	0.09	0.21	0.10	0.00
	0.04	*0.04*	*0.04*	*0.04*	*0.04*	*0.04*	*0.04*	*0.04*	*0.04*	*0.04*	*0.04*	*0.04*
(V+A+Z)/Chl*a+b*	0.46	0.06	0.11	**0.52**	0.24	0.15	**0.53**	0.25	0.16	0.33	0.24	0.03
	39.33	*61.01*	*59.07*	*43.41*	*54.44*	*57.66*	*42.77*	*54.06*	*57.39*	*51.22*	*54.77*	*61.72*
bulk car/Chl*a* +b	0.15	0.03	0.06	0.33	0.23	0.17	0.33	0.24	0.18	0.33	0.21	0.00
	0.08	*0.10*	*0.10*	*0.08*	*0.09*	*0.09*	*0.08*	*0.09*	*0.09*	*0.08*	*0.09*	*0.10*

Figure 1

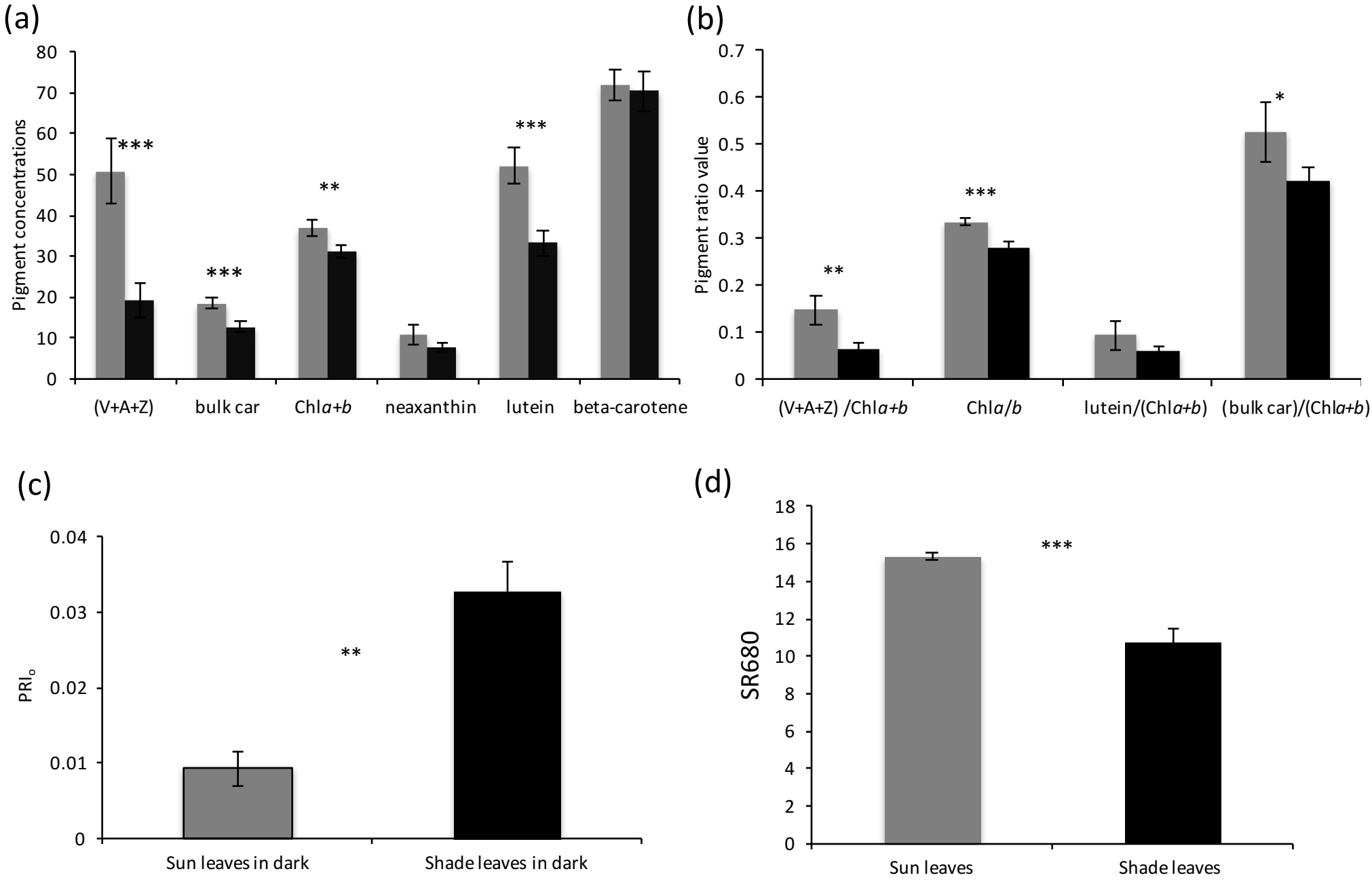
(a)
Pigment concentrations
80
70
60
50
40
30
20
10
0
***
***
**
***
(V+A+Z)
bulk car
Chl*a+b*
neaxanthin
lutein
beta-carotene
(b)
Pigment ratio value
0.7
0.6
0.5
0.4
0.3
0.2
0.1
0
**
***
*
(V+A+Z) /Chl*a+b*
Chl*a*/*b*
lutein/(Chl*a+b*)
(bulk car)/(Chl*a+b*)
(c)
PRI$_o$
0.04
0.03
0.02
0.01
0
**
Sun leaves in dark
Shade leaves in dark
(d)
SR680
18
16
14
12
10
8
6
4
2
0
***
Sun leaves
Shade leaves

Figure 2

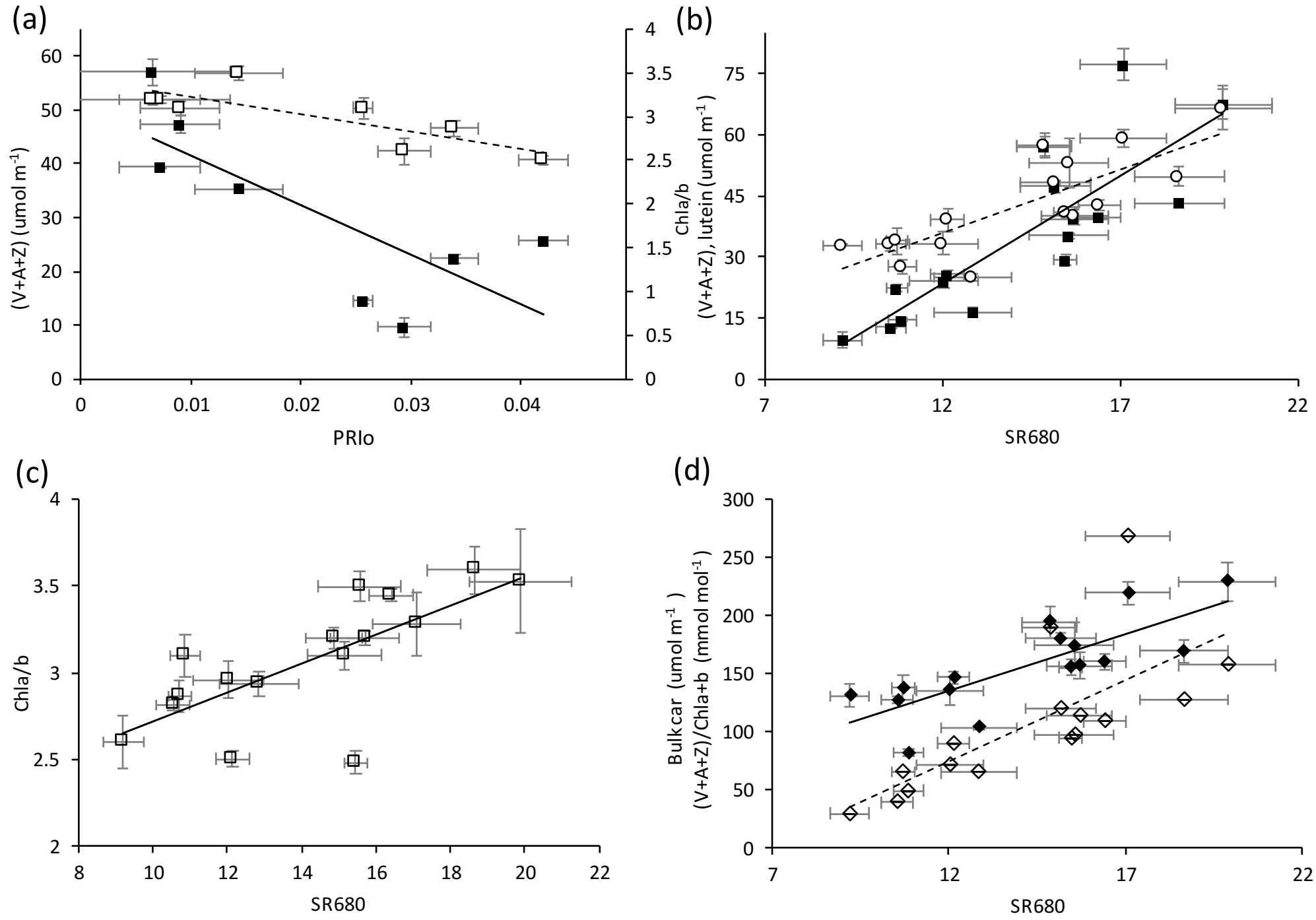
(a)
(V+A+Z) (umol m-1)
Chla/b
PRIo
(b)
(V+A+Z), lutein (umol m-1)
SR680
(c)
Chla/b
SR680
(d)
Bulkcar (umol m-1) (V+A+Z)/Chla+b (mmol mol-1)
SR680

Figure 3

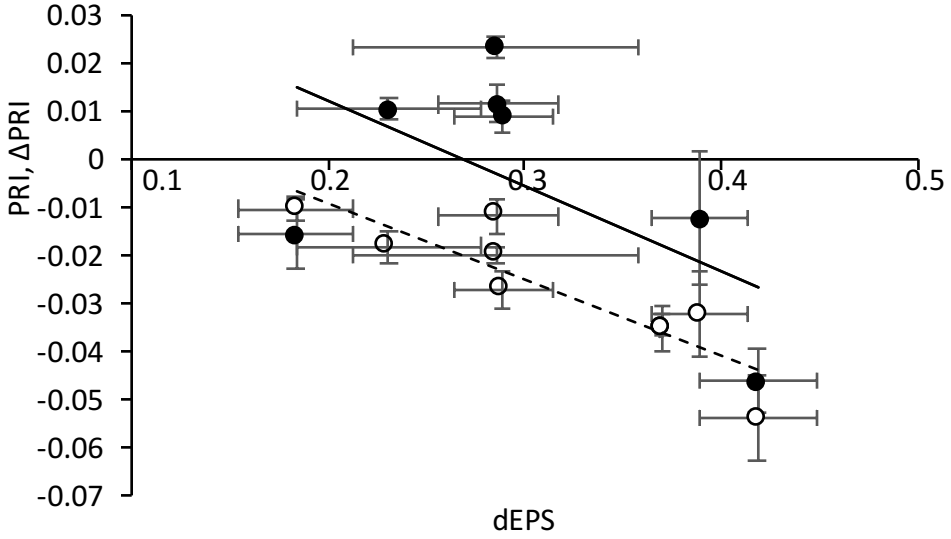
0.03
0.02
0.01
0
-0.01
-0.02
-0.03
-0.04
-0.05
-0.06
-0.07
PRI, ΔPRI
0.1
0.2
0.3
0.4
0.5
dEPS